
PREVENTING INFORMATION LEAKAGE WITH NEURAL ARCHITECTURE SEARCH

A PREPRINT

Shuang Zhang, Liyao Xiang, Congcong Li, Yixuan Wang, Zeyu Liu, Quanshi Zhang
Shanghai Jiao Tong University

Bo Li
The Hong Kong University of Science and Technology

May 31, 2022

ABSTRACT

Powered by machine learning services in the cloud, numerous learning-driven mobile applications are gaining popularity in the market. As deep learning tasks are mostly computation-intensive, it has become a trend to process raw data on devices and send the neural network features to the cloud, whereas the part of the neural network residing in the cloud completes the task to return final results. However, there is always the potential for unexpected leakage with the release of features, with which an adversary could infer a significant amount of information about the original data. To address this problem, we propose a privacy-preserving deep learning framework on top of the mobile cloud infrastructure: the trained deep neural network is tailored to prevent information leakage through features while maintaining highly accurate results. In essence, we learn the strategy to prevent leakage by modifying the trained deep neural network against a generic opponent, who infers unintended information from released features and auxiliary data, while preserving the accuracy of the model as much as possible.

Keywords Differential privacy · Mobile cloud · Neural networks

1 Introduction

The landscape of mobile computing has evolved with the recent move of deep learning algorithms from computational backends to the edge, with a number of optimized engines being readily available to application developers. Despite this trend, mobile devices are known for the lack of computational power, and thus not suitable for computation-intensive deep neural network (DNN) operations. Even a single inference step on mobile devices is at least 10 times slower than that on a computational server.

Instead of storing and processing the entire DNN on the device, a practical approach is to place the computation-intensive parts at the backend cloud. However, it would be a violation of privacy if we place the entire piece of DNN in the cloud and ask the user to upload raw data. Thus it becomes a design choice to select which features to be sent to the cloud for application performance while preserving data privacy. Such mobile-cloud computational frameworks have been adopted and discussed in [1, 2, 3, 4, 5].

Although the mobile-cloud computational framework brings performance gains compared to standalone computation on the device, it may lead to severe information leakage via the features released. It has been demonstrated that unintended information could be revealed by intermediate-layer representations in [6, 7, 8, 9], and worse still, attackers can even reconstruct inputs from the features they have access to [10, 11, 12].

As countermeasures, a number of approaches have been proposed, which roughly include two categories: differentially-private perturbation including [4, 13, 14, 15] as well as cryptographic methods such as [5, 16, 17]. Differentially-private mechanisms have been applied to the model parameters [13, 14], intermediate features [4], model predictions [15], or

objective functions [18]. For example, in [4], by nullifying sensitive regions of inputs and injecting random noise to the intermediate features, the device is able to guarantee strong privacy for any perturbed features sent to the cloud. Despite its strong privacy guarantee, it is unknown how the perturbed features can guard against any adversary attack. The methods rooted in cryptography are either computationally intensive, such as BGV homomorphic encryption schemes [5], or proposed under ideal two-party/three-party server assumptions [17]. Since the mobile device is mostly a thin piece with limited computation power, it is hard to meet the system requirements on model accuracy, storage, latency, power consumption, etc. in the implementation.

In view of the seemingly contradictory demands on user privacy and system performance, we resort to the DNN itself to seek a better balance between the two objectives. We observe that it is inherent to the neural network that its higher-level features tend to reveal less about the input, but simply offloading higher-level features to the cloud would gain us little performance advantage. Likewise, features of a compressed neural network reveal less about the input than features from a wider neural network, yet with a degraded accuracy level. Hence, it is a design choice to select which features to be sent to the cloud for optimizing the system performance as well as preserving user privacy. Such choices should be made *on demand*, since the performance of a mobile application may vary depending on the real-time state of the system. However, the choice is mostly difficult to make due to the huge search space, or subject to manual selection, as the relationship between the selection and the combined objective (privacy and system performance) is unclear. Moreover, an automatic feature selection framework which allows user-defined criteria is preferred as it would greatly benefit DNN-powered mobile applications.

We propose a novel feature selection and construction framework to automatically reshape the DNN intermediate-layer features to be sent from mobile devices to the cloud to optimize system performance while achieving the privacy-preserving goal. We select both the combinations of compression techniques and which layer of features to be sent to the cloud. The layer selected and the compression techniques constitute the new hyperparameters in our mobile cloud computational framework. To model customized user criteria on data privacy and system performance, we formulate the tuning of the hyperparameters as an optimization problem. Since the hyperparameter space is huge and seeking a closed-form solution is hard, we adopt a reinforcement learning (RL) based optimizer to search for the strategy to construct such intermediate-layer features to meet our performance objectives.

More specifically, our optimizer searches an encoder structure by cutting from a standard DNN and applying compression techniques to the DNN *stub* residing at the device. The encoder is trained together with the remaining parts of the DNN in the cloud to achieve a satisfactory level of accuracy and is also retrained to prevent a generic opponent who would try its best to reconstruct the inputs or infer sensitive input properties. Highlights of our work are as follows.

- As far as we know, the work is among the first that preserves user privacy from the neural network perspective, and in particular, the privacy metric is evaluated as the capability to guard against a generic adversary.
- We propose an RL-based optimizer which automatically searches for the best transformation and placement strategy of the neural network according to the user-defined criteria and platform resource constraints.
- We implement the optimizer and have it tested on a variety of models and datasets. The experimental results show its superiority in searching a neural network structure meeting the requirements of accuracy, privacy, and system performance at the same time.

2 Related work

The related works fall into the following three categories.

2.1 Running DNN with Mobile Devices

While DNN and deep learning algorithms have been widely applied, it still faces significant computational challenges when migrated to the thin mobile devices. A wide range of solutions has been proposed. From an *infrastructure* point of view, Lane *et al.* [19] were among the first to design a lower-power DNN inference engine on the device, taking advantage of both CPU and DSP chips to collaborate on mobile sensing and analysis tasks. Later in [2], Teerapittayanon *et al.* proposed to divide the DNN into different modules to deploy on the edge-cloud to improve the model accuracy and fault tolerance while keeping the communication cost low. Considering the resource constraints on the device, our work falls into the category of jointly deploying DNNs across mobile devices and the remote cloud to enhance running time performance.

Works such as [20, 21, 3, 22] delved into the *trade-off* between deploying an accurate model and satisfying system performance constraints. By applying intelligent data grouping and task formulations, Iyer *et al.* [21] resolved the accuracy and latency trade-off in troubleshooting radio access networks using machine learning techniques. Han *et al.*

[3] systematically traded off DNN classification accuracy for resource use by adapting to high workloads with less accurate variants of models. Similarly, Fang *et al.* [22] dynamically selects the optimal resource-accuracy trade-off for each deep learning model to fit the system’s available resources. By introducing the cloud into mobile deep learning, we could partially mitigate the resource-accuracy trade-off, but at the sacrifice of data privacy. Chi *et al.* [20] proposes an interactive adversarial training method against feature inversion attack without mentioning the impact of neural network architectures. Our work is among the first few that not only trains a neural network but also searches structures that fit best to our privacy objective.

2.2 Privacy Threats in Deep Learning

Abundant evidence has shown that the deployment of deep learning algorithms could potentially leak user privacy. Among them, we choose two typical privacy threats for investigation: feature inversion attack and property inference attack. The first category includes works such as [12, 10]. Mahendran *et al.* [12] proposed to recover the input by reconstructing intermediate-layer features while Dosovitskiy *et al.* directly reconstructed the input from features. Both of the works formulated the reconstruction as an optimization problem. It has been demonstrated that a significant part of the input can be recovered even from features merely with high-level semantic information.

Examples of the second category include the following. Membership inference attacks [6] could adversarially distinguish if a specific data record was used in training by exploiting the shadow models. Passive inference attacks [7] inferred unintended global properties of the training set merely from the trained models. Feature leakage in collaborative learning [8, 9] pointed out that the adversary could infer properties of a subset of the training data in the process that multiple users jointly train a global model. Until recently, there is no effective defense against the above two attacks, and our work proposes no defense but rather seeks a neural network structure that meets users’ privacy requirements against the two attacks.

2.3 DNN Compression

Our work is also related to a variety of DNN compression techniques. In [23], Han *et al.* proposed to prune unimportant model weights to compress the neural network. Along with quantization, their method has reduced the neural network size by 35 times with almost no accuracy degradation. Unlike non-structured pruning in [23], structured pruning kept the layer-wise structures intact but shrank the size of the neural network by removing the entire layer or scaling down the kernel size or the filter number [24]. Targeted at a number of mobile platforms, Liu *et al.* [25] trimmed down the network complexity with a number of compression techniques to satisfy resource constraints. While previous works mostly addressed the model accuracy and compression ratio, user privacy was rarely mentioned. Our work taps into this line of work to explore the relationship between neural network structures and user data privacy.

3 Preliminaries

In this section, we will give a brief overview of the techniques adopted in this paper.

3.1 Architecture Search

Until now, the architecture of most neural networks are subject to manual selection, but there is an on-going trend to automatically search for optimal neural network structures, of which the accuracy could match the hand-designed one. However, automatic search faces significant challenges when the state space is huge and the choice of the search space largely determines the difficulty of our problem. It is often critical to design the action space so that the optimization method can effectively search in the state space. To address this issue, we propose to compress a large neural network to a small one rather than growing one from scratch to shrink the search space.

A number of search strategies can be used to explore the search space, such as random search, Bayesian optimization, evolutionary methods, reinforcement learning, and gradient-based methods. Among them, reinforcement learning shows competitive accuracy and efficiency. Hence we adopt a reinforcement learning-based approach and carefully design its action space, state space, and reward function to effectively search for an optimal policy to find a desired DNN architecture.

3.2 Reinforcement Learning

Reinforcement learning is mostly concerned with how software agents take actions in an environment so as to maximize the cumulative reward. At each state, the agent takes action and communicates with the environment, which returns

new observation and reward for the current state and action. The agent adapts its policy which returns a new action and the action would lead to a new state of the agent. The objective of the agent is to learn an optimal policy to maximize the reward accumulated in the long run.

Since the optimal policy is far too complicated to find, many methods are proposed to approximate one. For example, there are value-based methods, policy-based methods and combined methods like Actor-Critic. In our work, we adopt Monte-Carlo policy gradient, a simple version of policy-based method, to search for the optimal DNN structure and placement strategy across the edge and the cloud.

4 Framework Overview

We aim to design a decision engine that tailors a conventional DNN to the mobile-cloud computational framework according to some customized requirements as well as resource constraints on the device. The decision engine is trained offline meeting different criteria sets by the application developer. When a user tries to run inference over DNN across the mobile device and the cloud, it can select from a variety of settings that meets its criteria. At its core, the decision engine consists of three modules: a DNN pool, a metric evaluator, and an optimizer. The relation between different components can be found in Fig. 1.

The DNN pool contains most of the up-to-date standard deep neural networks pre-trained, where we pick our base models from. Given the base model as its input, the optimizer makes the decision on which layers to retain on the device and which layers to offload to the cloud, as well as the compression techniques applied per layer on the device. The output of the optimizer is given in a form of hyperparameters, according to which the base model is modified and retrained w.r.t. several metrics. The hyperparameters are tuned by the reinforcement learning based optimizer in each episode to optimize the metrics include accuracy, privacy, storage, etc. Accuracy and model storage can be obtained easily from the tailored model, whereas privacy is evaluated using the best performance that an adversary achieves with two state-of-the-art attack techniques, *i.e.*, the feature inversion attack and property inference attack. For presentation compactness, we refer to the modified DNN stub on the device as *encoder*, and the attacker’s neural network as *decoder*. In a nutshell, our decision engine produces an encoder which 1) satisfies the mobile system requirement at runtime, 2) yields accurate output when used together with the DNN at the cloud for inference, and 3) preserves input privacy from the adversary.

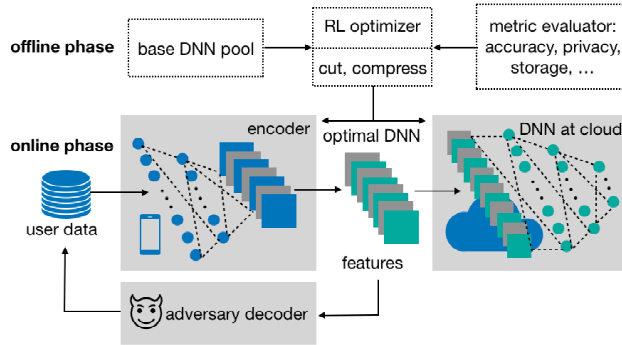


Figure 1: Framework overview.

Design space. To summarize, given a base DNN, we aim to search for an optimal strategy to *divide* and *compress* the DNN to obtain a DNN structure spanning across the mobile device and the cloud. Such a structure would meet our requirements on *model accuracy*, *data privacy*, and *system performance*, which we will illustrate in detail in the following section.

5 Formulation

As we have shown earlier, accuracy, privacy, and system performance are seemingly conflicting goals to achieve within one neural network. Hence, we aim to search for an optimal DNN structure and placement to find a sweet spot in between these objectives. In this section, we will illustrate how we measure or evaluate each metric in our framework.

We define a dataset with m examples as $D = \{(\mathbf{x}_1, y_1), \dots, (\mathbf{x}_m, y_m)\}$, where $\mathbf{X} = \{\mathbf{x}_1, \dots, \mathbf{x}_m\}$ denotes the set of input images and $\mathbf{y} = \{y_1, \dots, y_m\}$ is the corresponding true label. We use images as example studies but similar metrics can be applied to other cases. The parameters of the encoder e and the DNN stub at the cloud c are collectively

represented as θ_e and θ_c . The intermediate features output by e is expressed as $\mathbf{M} = f_e(\mathbf{X}; \theta_e)$ whereas c takes the features \mathbf{M} as inputs, and outputs predictions $\hat{\mathbf{y}} = f_c(\mathbf{M}; \theta_c)$. The **accuracy** performance is evaluated both on θ_e and θ_c such that:

$$A = 1 - \sum_i 1[\hat{y}_i \neq y_i]/m = 1 - \sum_i 1[f_c(f_e(\mathbf{x}_i; \theta_e); \theta_c) \neq y_i]/m \quad (1)$$

Note that accuracy has nothing to do with where we divide between e and c as long as the two parts are trained jointly as an entirety.

We propose to evaluate **privacy** by how much a generic adversary could infer any additional information about \mathbf{M} beyond what contains in \mathbf{y} . We introduce two categories of attack to the intermediate-layer features by summarizing from the current literature, but cannot claim it is a complete list.

Feature inversion attack. In this category of attack, the adversary tries to reconstruct the original input from features as in [10, 11, 12]. For example, Dosovitskiy *et. al.* [10] uses an up-convolutional network to invert features to minimize the mean squared error (MSE) of the reconstruction result. We implement the strategy and train a decoder on auxiliary dataset \mathbf{X}^a as follows:

$$\theta_{d1}^* = \arg \min_{\theta_{d1}} \sum_{\mathbf{x}_i \in \mathbf{X}^a} \|\mathbf{x}_i - f_d(f_e(\mathbf{x}_i; \theta_e); \theta_{d1})\|_2^2. \quad (2)$$

Given θ_{d1}^* , we are able to evaluate the privacy loss as the extent that the set of inputs are reconstructed on \mathbf{X}^a :

$$P_0 = 1 - P'_0 / \max P'_0, \quad (3)$$

where $P'_0 = \mathbb{E}[\|f_d(f_e(\mathbf{x}_i; \theta_e); \theta_{d1}^*) - \mathbf{x}_i\|_2]$. The closer the decoder reconstructs the original input, the higher the privacy loss. Some argue that the structural similarity index (SSIM) [26] is a better indicator of the similarity between two images than the MSE, as SSIM mimics the human visual system highly adapting to extract structural information from the viewing field. The SSIM we adopted in this paper separate out three factors — luminance, contrast, and structure — to yield an overall similarity measure. For more detail, please refer to [26]. Hence, the opponent would devise a decoder to reconstruct the input with the highest SSIM:

$$\theta_{d1'}^* = \arg \max_{\theta_{d1'}} \sum_{\mathbf{x}_i \in \mathbf{X}^a} \text{SSIM}(\mathbf{x}_i, f_d(f_e(\mathbf{x}_i; \theta_e); \theta_{d1'})). \quad (4)$$

Likewise, we define the privacy loss as the similarity metric:

$$P_1 = \mathbb{E}[\text{SSIM}(\mathbf{x}_i, f_d(f_e(\mathbf{x}_i; \theta_e); \theta_{d1'}^*))]. \quad (5)$$

Note that the value of SSIM always lies between 0 and 1.

Property inference attack. In this category, the adversary infers from features about the input properties beyond what contains in the output, as in works such as [6, 7, 8]. That indicates the adversary capability of deducting additional information irrelevant to the task. For example, let the task being the classification of a person's age ranges based on its facial image. And we would not expect any party to learn anything beyond that. However, an adversary intends to infer an unrelated attribute, *i.e.*, the gender of the person, from the released features somehow. Hence, it secretly collects a set of person images with different genders \mathbf{X}^a and their corresponding features $f_e(\mathbf{X}^a; \theta_e)$. The adversary trains a binary classifier θ_{d2}^* to distinguish the attribute of genders \mathbf{y}^a that:

$$\theta_{d2}^* = \arg \min_{\theta_{d2}} \sum_{\mathbf{x}_i \in \mathbf{X}^a} 1[f_d(f_e(\mathbf{x}_i; \theta_e); \theta_{d2}) \neq y_i]. \quad (6)$$

Such a binary classifier is used to infer the hidden gender property from features, by which we define privacy loss as the inference accuracy on the unintended attributes:

$$P_2 = \sum_{\mathbf{x}_i \in \mathbf{X}^a} 1[f_d(f_e(\mathbf{x}_i; \theta_e); \theta_{d2}^*) = y_i] / |\mathbf{X}^a|, \quad (7)$$

where $|\mathbf{X}^a|$ is the total number of instances in \mathbf{X}^a . Overall we try to mimic the real-world privacy threats to provide insights on how the neural network architecture design would affect the privacy performance. In practice, we cannot control what the adversary obtains in the auxiliary dataset \mathbf{X}^a , and thus we assume a worst-case adversary who exploits whatever it has.

Apart from accuracy and privacy, the running time **performance** is also one major factor in consideration, as it concerns with user experience, *i.e.*, how fast the DNN processes the data (latency), how large space it takes (storage), and how much energy it consumes (energy). All these factors are relevant to the amount of computation on the device: a deeper or wider DNN stub takes larger storage space and most often involves more computation leading to longer inference

time as well as higher energy consumption. For simplicity, we adopt the following *performance indicators* to denote the running time performance:

$$S_1 = 1 - \frac{\#\text{params}(\text{encoder})}{\#\text{params}(\text{total})}, \quad (8)$$

and in the case where FLOPs cannot be estimated by the number of parameters, we adopt

$$S_2 = 1 - \frac{\text{MACs}(\text{encoder})}{\text{MACs}(\text{total})}. \quad (9)$$

MACs are approximated by the sum of MACs in the convolutional and fully-connected layers as follows:

$$\text{MACs}_{\text{conv}} = K \times K \times C_{in} \times C_{out} \times H_{out} \times W_{out} \quad (10)$$

$$\text{MACs}_{\text{FC}} = C_{in} \times C_{out} \quad (11)$$

where K represents the kernel size, H_{out}, W_{out} are the height and width of output feature, and C_{in}, C_{out} denote the number of input and output channels of the layer.

Essentially, with a larger S_1/S_2 , the storage or computation costs on the mobile device are lower, with more workload transferred to the cloud. We certainly can use a more complex latency or energy model for better describing the performance gain, but that is out of the scope of this work.

To sum up, *accuracy* A is evaluated on the model jointly composed by the encoder and the DNN at the cloud. *Privacy loss* P_0, P_1, P_2 are defined as the amount of unintended information contained in the features released. The worse the adversary’s performance in recovering inputs or inferring unintended properties of the input, the higher level of privacy the mechanism guarantees. *Performance indicator* S_1, S_2 are concerned with both the compression ratio and partitioning strategy. Among these metrics, privacy and accuracy are related to both model parameters and hyperparameters, while the performance indicator is mostly relevant to hyperparameters such as the number of parameters per layer, layer type, input size, etc. In the following section, we will introduce our reward objective function composed of the metrics and the strategy design space.

6 Reinforcement Learning Based Optimizer

Our goal is to learn the optimal partition and transformation strategy (policy) π^* via reinforcement learning, of which the major components are as follows:

State: Let the state space \mathcal{S} be the one containing all neural network models along with its placement on devices. Each model is represented by a set of hyperparameters and model weights. For example, a state can be the first 3 convolutional layers (Conv-layers) residing at the mobile device, with the following 2 Conv-layers and the fully-connected layers placed at the cloud. It would be a different state if the same model is deployed but only the first 2 Conv-layers are assigned to the device.

Action: A finite action set \mathcal{A} transforms a state from one to another. We consider two types of actions in this work: the *partition* of the model across different devices, and model *compression*. By compressing a base DNN to one fitting the mobile end, it not only shrinks down the search space but with some accuracy guarantee by the conclusion of [23].

Transition probability and discount factor: Letting the transition probability space be \mathcal{T} , we take a deterministic approach to transform a DNN structure from one to another with probability 1. And we set the discount factor γ to 1 to make each reward contribute equally to the final return.

Reward function: The reward $r : \mathcal{S} \mapsto \mathbb{R}$ can be factorized as model accuracy, privacy, and performance indicator aforementioned. After taking each action, we obtain a new state — a new DNN structure and its placement — along with its associated reward. To explore more DNN structures at one run, we generate more than one new DNN within each episode and use their average reward as the reward for the action taken. Note that with each action taken, not all metrics would change. For instance, the action of partition does not change the model accuracy or the performance indicator, while compression would affect all metrics. Further, we define the intermediate reward to be zero, *i.e.*, the reward should only be given when the compression procedure is done for all layers, and any intermediate state would be rewarded 0.

We consider a large reward should be given when the model achieves a high level of all three metrics. If all three metrics are treated equivalently, we can express the reward in the following form:

$$R = R_A \times R_P \times R_S = \frac{A}{A_{\text{base}}} \times (1 - P_i) \times S_j(2 - S_j), \quad i \in \{0, 1, 2\}, j \in \{1, 2\}. \quad (12)$$

R_A, R_P, R_S are all normalized between the value of 0 and 1. With A_{base} expressed as the accuracy of the base DNN, R_A indicates the ratio between the accuracy of the optimal DNN and the baseline accuracy. Similarly, R_P is the negative of privacy loss. The reward R_S is expressed as a concave function of S_j as we assume the performance gain grows drastically when S_j is small but becomes marginal when S_j is close to 1.

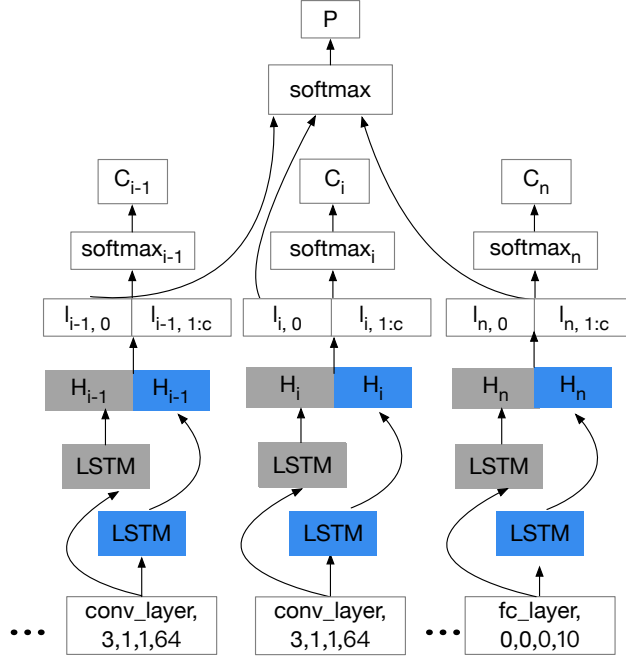


Figure 2: Reinforcement learning based optimizer. C_i represents the compression policy of the i -th layer and P represents the partition policy.

6.1 LSTM-based Optimizer

Since recurrent neural networks have been widely applied to neural architecture search, for their capability to process hyperparameters expressed as strings. We adopt the bidirectional LSTM, a type of recurrent neural network, as the decision engine in our reinforcement learning optimizer.

The structure of the decision engine is given by Fig. 2. The basic unit is a DNN layer, which includes the in-place operations such as ReLU, batch normalization, dropout, etc. if it contains one. Each layer takes the current state of the layer as input, feeds them into a forward LSTM and a backward LSTM respectively to compute the corresponding hidden states H_i . As the change of one layer can affect the layer prior to it or the layer following it, the design of the backward and forward LSTM ensures such influence is reflected by the Q-network. The hidden states units produce a number of logits with respect to the partition decision I_0 and compression decision $I_{1:C}$ for each layer. For the partition decision, each logit I_0 can be interpreted as the preference of partitioning between the current layer and the following one. For the compression strategy, we consider each logit $I_{1:C}$ as each layer's preference over a set of compression techniques. Finally, I_0 across all layers are fed into one common softmax layer to produce the partition decision P , whereas $I_{1:C}$ are fed into the per-layer softmax to produce the set of compression techniques C_i for this layer. Given the produced actions $C_i, \forall i \in \{1, \dots, n\}$ and P , we are able to transform one DNN model to another along with the change of its placement, and thus transit to the next state.

6.2 Adversarial Retraining

For each set of hyperparameters (and the DNN placement) produced as the state, we compose a neural network according to those hyperparameters and re-initialize it for training. According to Eq. (12), the reward consists of R_A, R_P and R_S . While R_S can be obtained before retraining, the former two can only be evaluated after retraining.

In retraining the composed model, we adopt knowledge distillation for better accuracy performance. The technique labels the training dataset by probabilistic outputs (soft labels) of the corresponding base model, rather than the hard labels. By Hinton *et al.* [27], the probabilistic outputs emphasize on the relation between different classes and thus

provide more information than hard labels to assist training. In our framework, both hard and soft labels are adopted in the loss function.

As for calculating the privacy, we apply two retraining strategies w.r.t. different threat models. We first consider a *reactive* adversary who can only obtain whatever the user outputs from a trained encoder. In that model, the adversary manipulates the user by intentionally sending inputs to the encoder and retrieving the corresponding intermediate-layer features from it. By training a decoder over the obtained input-feature pairs, we record the best performance achieved by the decoder in terms of the input reconstruction error or the property inference error. Such errors are adopted to gauge the privacy level that the encoder can achieve.

Also, we assume a *proactive* attack in which the adversary can interact with the training of the composed DNN. In particular, at each iteration of retraining the composed DNN, the adversary trains a decoder against the current encoder to minimize the encoder’s privacy gain, and then with the decoder fixed, the encoder is trained to maximize its privacy gain and final output accuracy. In a nutshell, the encoder and decoder pit against each other to achieve a saddle point in the following minimax problem:

$$\min_{\theta_e, \theta_c} \max_{\theta_d} (1 - A) + P_i, \quad i \in \{0, 1, 2\}. \quad (13)$$

In the equation above, the model accuracy A is concerned with both θ_e and θ_c whereas the privacy loss P_i is a function of θ_e and θ_d . The formulation resembles the training of a generative adversarial network (GAN) where the encoder and decoder play the roles of discriminator and generator respectively. In practice, it is hard to train such a minimax loss as the decoder usually converges much faster than the encoder and the cloud. Thus we adopt similar training strategies as GANs to slow down the training of the decoder.

To sum up, in the reactive adversary model, as the user and the adversary are not aware of the encoding/decoding strategies of the other, both of them are weak: the user can only maximize the accuracy performance of the composed model but not know the privacy threat it will face. As to the proactive adversary model, both the user and the adversary are stronger: the adversary, being aware of the power of the user, trains a decoder to compromise the user privacy whereas the user not only seeks high accuracy but also satisfactory privacy performance against such an adversary.

6.3 Optimization

With the reward calculated for each state, we run the LSTM-based optimizer to find the optimal partition-compression policy. Policy π is represented by the LSTM-based network parameterized by w . At episode i , the policy is represented by $\pi(w_i)$. During each episode, we compute the action under the current state and policy, and transit to the next state. To facilitate computation, M samples are rolled out for the given policy to compute the expected reward.

Algorithm 1 Reinforcement Learning $(\mathcal{S}, \mathcal{A}, \mathcal{T}, r, \gamma)$

Input: a base DNN

Output: a new DNN and its placement

```

1:  $s_0 \leftarrow$  The base DNN;
2: for  $i = 1$  to  $N$  do
3:   for  $j = 1$  to  $M$  do
4:      $s_{j,0} = s_0$ ; {Set the initial state to  $s_0$ .}
5:     for  $t = 1$  to  $L$  do
6:        $a_{j,t} \sim \pi(s_{j,t-1}; w_{i-1})$ ;
7:        $s_{j,t} \leftarrow T(s_{j,t-1}, a_{j,t})$ ;
8:     end for
9:      $R \leftarrow \frac{1}{M} \sum_{j=1}^M r(s_{j,L})$ ; {Use the average reward for the current policy.}
10:     $w_i \leftarrow \nabla_{w_{i-1}} J(w_{i-1})$ ;
11:   end for
12: end for

```

Policy gradient method is used to update the policy in each episode. Specifically, the objective function for the policy network is the expected reward over all sequences of actions $a_{1:L}$, *i.e.*:

$$J(w) = E_{a_{1:L} \sim \Pi(w)}[R], \quad (14)$$

where L is the length of the trajectory. REINFORCE policy gradient algorithm [28] is applied to train the policy network. And we adopt a common trick called baseline to reduce the high variance in the gradient. Finally, Alg. 1 summarizes the reinforcement learning optimization procedure.

Table 1: Compression Techniques

Name	Replaced Structure	New Structure	Applied Layer Types
F_1 (SVD)	$m \times n$ weight matrix	$m \times k$ and $k \times n (k \ll m)$ weight matrices	FC layer
F_2 (KSVD)	same above	same above with sparse matrices	FC layer
F_3 (Global Average Pooling)	FC layers	a global average pooling layer	FC layer
C_1 (MobileNet)	Conv layer	3×3 depth-wise Conv layer and 1×1 point-wise Conv layer	Conv layer
C_2 (MobileNetV2)	Conv layer	same above with additional point-wise Conv layer and residual links	Conv layer
C_3 (SqueezeNet)	Conv layer	a Fire layer	Conv layer
W_1 (Pruning)	any layer	insignificant parameters pruned layer	FC or Conv layer
W_2 (Filter Pruning)	Conv layer	insignificant filters pruned Conv layer	Conv layer

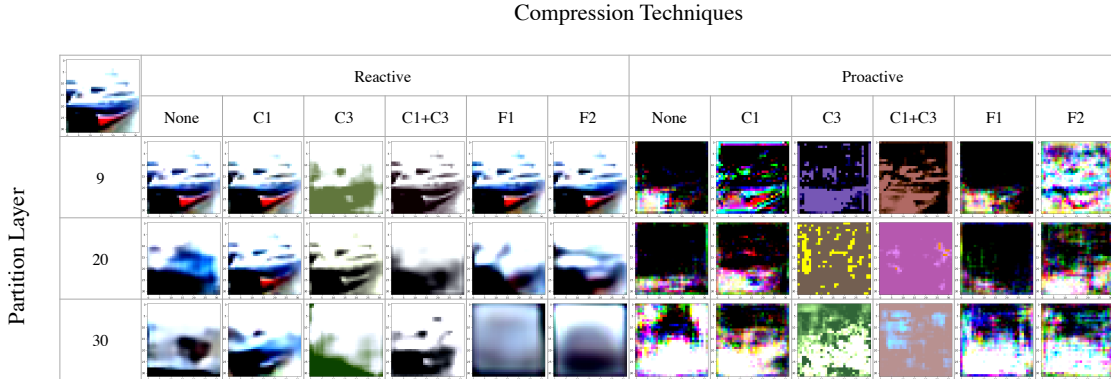


Figure 3: The visualization effect of reconstructed inputs reversed from different partitioning layers under a variety of compression techniques on VGG-13, CIFAR-10. Reactive means the decoder only passively reconstructs the input from features. Proactive means that the decoder and encoder pit against each other for retraining the model. We observe that the reconstruction effect is poor when the partitioning layer is close to the output layer, especially when the model is compressed. Proactive decoder has a worse reconstruction effect as the encoder is enhanced with retraining.

7 Evaluations

In this section, we show that our RL-based optimizer is able to find high-performance DNN structures achieving high accuracy while leaking little unintended information about the inputs. The experimental results and visualization effect on a variety of datasets and base neural networks demonstrate that the effectiveness of our method.

Setup: We choose the image classification tasks on CIFAR-10 and CIFAR-100 to test our RL-based optimizer. Base DNNs are the conventional models LeNet, AlexNet, VGG-11, VGG-13 and VGG-16. The decoder has an inverse structure as of the encoder. The task on CIFAR-10 is to classify the 10-class color images and to prevent the *feature inversion attack*. For any DNN selected by our strategy, we evaluate its accuracy by the classification error and privacy by the MSE and SSIM of the reconstructed inputs. The task on CIFAR-100 is to classify the images into 20 superclasses while not disclosing the fine class of each image. We evaluate the model accuracy by the classification accuracy of 20 superclasses attributes, and privacy by the classification error rate of the fine-class attributes. The latter can be considered as preventing *property inference attack*.

We implement the most common compression techniques as listed in Table 1. The RL-based optimizer is implemented by the machine learning framework PyTorch 1.1.0 and all experiments are done on Intel Xeon Processor with GPU GeForce RTX 2080 Ti.

7.1 Implementation Details

In this section, we first introduce our two types of RL-based optimizers and then show the comparison methods.

RL-based Optimizer (reactive): The RL algorithm is trained for 200 episodes with a learning rate of 0.03 and a rollout number 1. Within each episode, after applying the partition and compression techniques to the encoder, we retrain the new model to minimize the accuracy loss for 1 epoch with a learning rate 0.001, and train the reactive decoder for 1 epoch with the same learning rate to minimize the privacy loss which is indicated by MSE or the negative value of SSIM. After recording the reward and updating the controller, the next episode begins.

RL-based Optimizer (proactive): Similar to that with reactive adversary, within one episode, we partition and compress the DNN, and construct the decoder with an inverse structure of the encoder. We first train the cloud part for 5 epochs to minimize the model’s accuracy loss, and then train the decoder for 1 epoch to minimize the privacy loss. Finally, we train the encoder for 5 epochs to minimize the accuracy loss and maximize the privacy loss at the same time, and then repeat the entire procedure for the next episode. We observe that 200 episodes are sufficient to find the saddle point. The training strategy is sufficient for the controller to distinguish different compressed models while not being overburdening. The learning rates of the partition controller and compression controller are both set as 0.03 and the rollout number is 1.

Comparison Methods: We first verify that RL-based optimizer exceeds other neural architecture search methods in terms of performance. We adopt the grid search as a comparison method which computes the highest reward out of all combination choices of partitioning layers and compression techniques. Note that doing an exhaustive search over all choices is almost impossible (due to the difficulty for reward computation). Two adversarial training strategies also apply to the grid search.

Beyond that, we also compare our approach against other privacy-preserving method — *differential privacy*, which adds additional Gaussian noise to the intermediate-layer features at the inference phase. The random noise is drawn from Gaussian distributions with 0 mean and standard deviation 0.1, 0.5, 1, 2 times of the mean magnitude of the features respectively. We would like to show that, with our adaptation of the neural network, goals of accuracy, privacy, and performance can be better achieved.

Table 2: Different compression techniques lead to different compression ratios and accuracies on AlexNet, CIFAR10.

A_{base}	Compression Techniques	CR	A	ΔA
0.8679	10:C1	0.0224	0.8538	-1.62%
	3:C3 6:C3 8:C3 10:C3	0.0859	0.8291	-4.47%
	0:W1 3:W1 6:W1 8:W1 10:W1	0.0645	0.8393	-3.30%
	0:W1 3:W1 6:W1 8:W1 10:C1	0.0701	0.8251	-4.93%
	0:W2 3:W2 6:W2 8:W2 10:C1	0.0743	0.8153	-6.06%

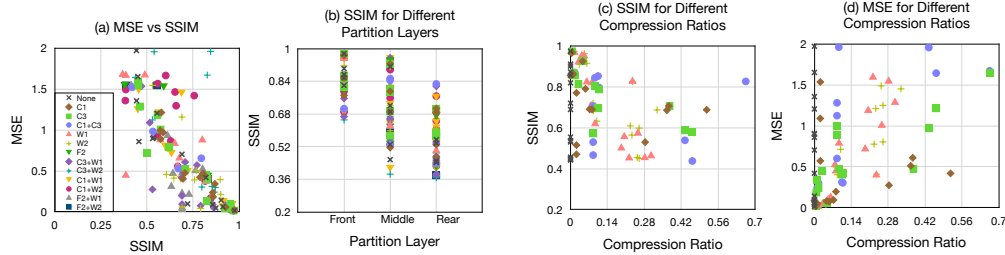


Figure 4: The impact of different compression and partition strategies on privacy measured by SSIM and MSE on CIFAR-10. Figures share the same legend. (a): SSIM and MSE are negatively correlated. (b): SSIM is lower when the partition layer is closer to the output layer of the model. (c)(d): SSIM (MSE) is higher (lower) when compression ratio is low.

7.2 Results and Discussion

We first verify the impact of different compression techniques on neural networks, and then show the adversarial retraining and the training process of reinforcement learning. Finally, we compare our search results with other methods.

Accuracy and Privacy vs. Compression and Partition. *Compression Ratio* is defined as

$$CR = 1 - \frac{\#params(compressed\ DNN)}{\#params(base\ DNN)}$$

to indicate how much the model is compressed. We take AlexNet for example: when we divide AlexNet at the 12th layer and apply different combinations of compression techniques up to that layer, we obtain different CRs and accuracies as shown in Table 2. Further, from Fig. 4, we can tell that choices of partition layers and compression ratios have different impact to the privacy performance. Data are collected from models including VGG-11, VGG-13, VGG-16, LeNet, AlexNet, and ResNet-18. Remarkably, features closer to the input layer, or with a lower CR, tend to better reconstruct the inputs and thus reveal more.

We also display the visualization effect of each reconstructed input restored from different features in Fig. 3. From left to right, each image is reconstructed from features compressed by different techniques, when reactive or proactive training

are applied. From top to bottom, each image is reconstructed from different partitioning layers. Overall, features closer to the input layer have a better reconstruction effect, and one can hardly reconstruct input from proactively trained features. The latter shows in proactive training, the encoder gradually learns how to shield information from the decoder. Above all, different compression techniques and partitioning strategies indeed have various impacts on the accuracy and privacy performance of a model.

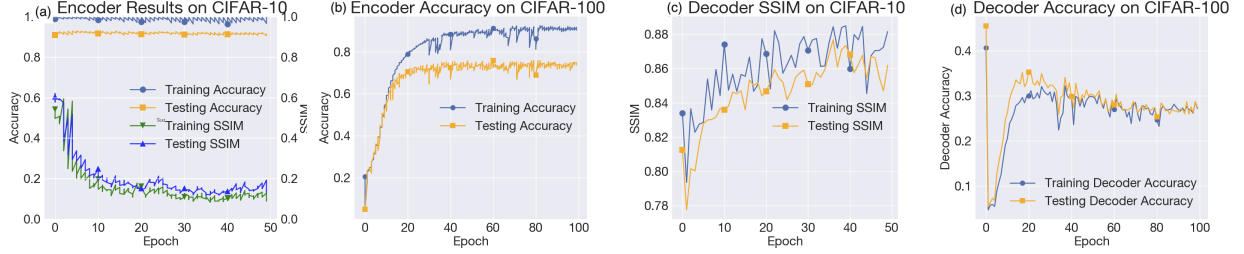


Figure 5: We partition VGG-16 at Layer 13 (left) and at Layer 33 (right), and then use filter pruning to compress the encoder. On the left side, the proactive decoder tries to maximize the SSIM to reconstruct the inputs. On the right side, the proactive decoder tries to minimize its classification error on the fine-class attributes to infer input properties.

Adversarial Retraining. Fig. 5-(a)(c) demonstrate an example proactive retraining process on CIFAR-10, VGG-16. As we observe, the overall model accuracy is high and stable throughout the training process, while the decoder and encoder pit against each other on the privacy loss with the encoder at an advantage. Fig. 5-(b)(d) shows the proactive retraining on CIFAR-100, VGG-16. The decoder accuracy decays at the 20th epoch as the encoder gets stronger. The overall model accuracy remains stable.

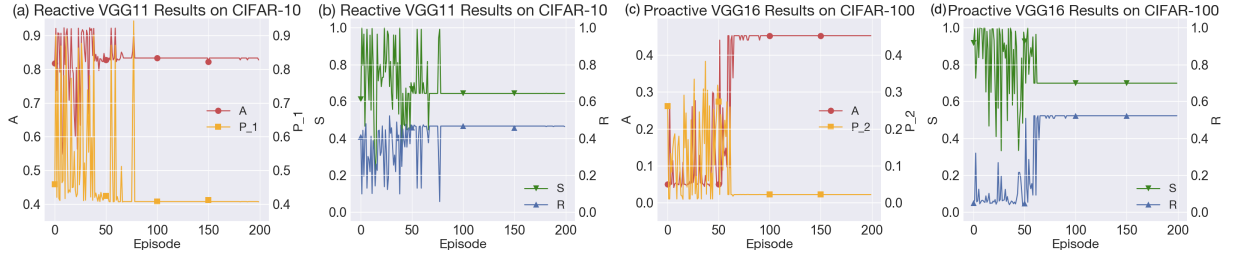


Figure 6: The reinforcement learning processes of training VGG-11 on CIFAR-10 with the reactive decoder (a)(b), and training VGG-16 on CIFAR-100 with the proactive decoder (c)(d).

Reinforcement Learning. Fig. 6 show the convergence of our RL-based optimizer. We follow the notations in Sec. 5 in presenting the results. From Fig. 6(a)(c), the model accuracy remains stable throughout the learning process, while SSIM and the decoder accuracy decreases indicating an increase of the privacy level. That essentially suggests our optimizer learns to select neural network structures and features which preserves input privacy without degrading the model performance. Fig. 6(b)(d) show that the rewards increase with episodes until convergence.

Comparison with Grid Search. Table 3 shows our reinforcement learning based optimizer approach and as a comparison, we did a grid search over the same search space, of which the results are given in Table 4. In both tables, we show the strategies the two methods find out, and the resulting models’ accuracy A , privacy loss $P_1(P_2)$, performance indicator $S_1(S_2)$ and reward R . Our RL-based optimizer achieves the highest reward in almost all cases, with an average improvement of 8.35% over the grid search. While the model accuracies remain almost the same (with moderate decreases in some cases), our privacy loss reduces by 13.22% on average compared to grid search. The results demonstrate the effectiveness of RL-based optimizer in seeking neural network structures and placement which preserve input privacy.

Comparison with Differential Privacy. To verify the strength of adapting neural network structures to privacy goals, we also compare our approach against another privacy-preserving method. Differential privacy, as a conventional method, inserts randomized noise to the partitioning layer without modifying the neural network structures. The perturbed features are expected to preserve input privacy. Results are given in Table 5. To compare with Table 3, we also calculate the performance indicator S_1 , privacy loss P_1 and reward R of each model accordingly. In general, feature perturbation reduces privacy loss over the base level, and the larger the standard deviation of the noise, the lower

Table 3: Results of running reinforcement Learning based optimizer over different models and datasets: $\Delta_g R$, $\Delta_g P_1(\Delta_g P_2)$ are the reward gain and privacy loss reduction over the grid search method. $\Delta_n R$, $\Delta_n P_1(\Delta_n P_2)$ are the reward gain and privacy loss reduction over the differential privacy method. The results show that our method is superior in seeking a model structure that achieves a high reward and low privacy loss.

	Model	Partition Layer	Compression Techniques	A	$P_1(P_2)$	$S_1(S_2)$	R	$\Delta_g R$	$\Delta_g P_1(\Delta_g P_2)$	$\Delta_n R$	$\Delta_n P_1(\Delta_n P_2)$
CIFAR-10 Reactive	VGG11	23	18:C2 22:C1	0.9108	0.4106	0.6808	0.5218	19.65%	-22.53%	87.70%	-35.36%
	VGG13	0	0:C1	0.8298	0.3867	0.9999	0.5401	6.28%	-14.82%	36.63%	-18.49%
	VGG16	40	0:W1 3:W1 7:W1 10:W1 14:W1 17:W1 20:W1 24:W1 27:W1 30:W1 34:C1 37:C1 40:W1	0.9213	0.4049	0.7369	0.5430	1.08%	-10.56%	15.93%	-12.47%
	AlexNet	13	8:W1 10:W1	0.8657	0.3803	0.9455	0.6163	3.49%	-1.35%		
	Lenet	5	3:C3	0.7502	0.5300	0.9537	0.4678	5.41%	2.00%		
	AlexNet (S_2)	10	6:W2 8:W2 10:W2	0.8524	0.3803	0.9099	0.6037	8.42%	-8.18%		
CIFAR-10 Proactive	Lenet (S_2)	10	0:W2 3:W2	0.6051	0.3806	0.8356	0.4848	17.16%	-31.21%		
	VGG11	13	0:C1	0.8344	0.3948	0.8959	0.5405	4.89%	-3.64%	94.42%	-37.85%
	VGG13	26	0:C3 14:W1 21:W1 24:C3	0.8534	0.3997	0.8294	0.5279	2.98%	4.55%	34.22%	-15.75%
	VGG16	44	3:W2 10:W2 14:W2 17:W2 20:W2 24:W2 27:W2 30:W2 34:W2 37:W2 40:W2	0.9173	0.4160	0.6953	0.5171	-4.42%	-1.75%	10.40%	-10.07%
CIFAR-100 Proactive	VGG11 (P_2)	3	none	0.7176	0.1706	0.9998	0.7876	2.03%	31.03%		
	VGG13 (P_2)	33	0:W2 3:W2 7:W2 14:W2 17:W2 21:W2 24:W2 28:W2 31:W2	0.6387	0.037	0.6882	0.7237	18.83%	-89.55%		
	VGG16 (P_2)	1	none	0.7741	0.1781	0.9997	0.8251	22.71%	-25.95%		

Table 4: Results of grid search over different models and datasets.

	Model	Partition Layer	Compression Techniques	A_{base}	A	$P_1(P_2)$	$S_1(S_2)$	R
CIFAR-10 Reactive	VGG11	21	11:C1 18:C1	0.9241	0.8950	0.5300	0.7950	0.4361
	VGG13	30	0:W1 3:W1 7:W1 10:W1 14:W1 17:W1 21:W1 24:W1 28:W1	0.9423	0.9353	0.4540	0.7502	0.5082
	VGG16	33	0:W1 3:W1 7:W1 10:W1 14:W1 17:W1 20:W1 24:W1 27:W1 30:W1	0.9397	0.9282	0.4527	0.9200	0.5372
	AlexNet	16	0:W1 3:W1 6:W1 8:W1 10:W1 14:F1	0.8679	0.8425	0.3855	0.9587	0.5955
	LeNet	7	6:F1	0.7522	0.7189	0.5196	0.8176	0.4438
	AlexNet (S_2)	12	0:W1 3:W1 6:W1 8:W1 10:C1	0.8679	0.8251	0.4142	0.9867	0.5568
CIFAR-10 Proactive	LeNet (S_2)	7	0:W1 3:W1 6:W1	0.7522	0.7096	0.5533	0.8661	0.4138
	VGG11	14	0:C3 4:C3 8:C3 11:C3	0.9241	0.8227	0.4097	0.8609	0.5153
	VGG13	20	0:C3 3:C3 7:C3 10:C3 14:C3 17:C3	0.9423	0.7974	0.3823	0.8613	0.5126
	VGG16	33	0:W1 3:W1 7:W1 10:W1 14:W1 17:W1 20:W1 24:W1 27:W1 30:W1	0.9397	0.9090	0.4234	0.8269	0.5410
CIFAR-100 Proactive	VGG11 (P_2)	21	0:W1 4:W1 8:W1 11:W1 15:W1 18:W1	0.7557	0.6889	0.1302	0.8372	0.7719
	VGG13 (P_2)	30	0:W1 3:W1 7:W1 10:W1 14:W1 17:W1 21:W1 24:W1 28:W1	0.7673	0.7717	0.3542	0.7502	0.6090
	VGG16 (P_2)	33	0:W2 3:W2 7:W2 10:W2 14:W2 17:W2 20:W2 24:W2 27:W2 30:W2	0.7711	0.6998	0.2405	0.8437	0.6724

Table 5: Results of applying differential privacy to the models: randomized Gaussian noises are inserted to the selected partitioning layers. Base privacy loss is calculated on the original models and features. The mean of the inserted Gaussian noise is 0, and the standard deviation is set to 0.1, 0.5, 1, and 2 times of the average feature magnitude. Reward R is calculated according to Eq.12 for fair comparison.

	Partition Layer	Base Privacy Loss	S_1	$P_1(0.1x)$	$R(0.1x)$	$P_1(0.5x)$	$R(0.5x)$	$P_1(1x)$	$R(1x)$	$P_1(2x)$	$R(2x)$
CIFAR-10 VGG11	7	0.9713	0.9918	0.9654	0.0346	0.9274	0.07267	0.9328	0.0672	0.8486	0.1514
	14	0.8747	0.8958	0.8571	0.1414	0.8700	0.1286	0.8531	0.1453	0.8461	0.1522
	21	0.7089	0.5122	0.7054	0.2245	0.6905	0.2358	0.6659	0.2546	0.6352	0.2780
CIFAR-10 VGG13	9	0.9401	0.9880	0.9587	0.0413	0.9460	0.0540	0.9106	0.0894	0.9074	0.0926
	20	0.7904	0.8782	0.7947	0.2023	0.7999	0.1972	0.7811	0.2157	0.7752	0.2215
	30	0.5272	0.5020	0.5116	0.3672	0.5060	0.3715	0.4900	0.3835	0.4744	0.3953
CIFAR-10 VGG16	13	0.9095	0.9823	0.9153	0.0847	0.8953	0.1047	0.8913	0.1086	0.8813	0.1186
	23	0.7197	0.9221	0.7516	0.2468	0.7545	0.2440	0.7626	0.2359	0.7281	0.2703
	33	0.5211	0.6416	0.5144	0.4233	0.5182	0.4199	0.4998	0.4360	0.4626	0.4684

the privacy loss. Interestingly, we found that while P_1 decreases with an increase of the noise standard deviation, R increases with it. That shows our reward function is well designed to reflect our privacy objective.

We choose the group with the highest reward ($2x$ standard deviation) to compare with the RL-based approach. The results are provided in Table 3. On average, the RL-based approach exceeds differential privacy by 46.43% in reward, with a reduction of 21.67% in privacy loss. The result confirms that modifying the neural network structure can achieve a higher level of privacy compared with feature perturbations.

8 Conclusion

For deep learning with the mobile cloud infrastructure, we propose to protect the sensitive information in the input data from the perspective of the neural network. By proper partition, compression, and adversarial retraining, the neural network can be adapted to yield far less privacy loss without much performance degradation. To achieve that, we devise a reinforcement learning based optimizer to seek the best adaptation strategies. Although we formulate it as an unconstrained optimization problem, it can be easily revised to a constrained optimization problem if a hard privacy

guarantee is imposed. Experiments on various model structures have shown that the RL-based approach exceeds that of grid search, as well as other privacy-preserving method such as differential privacy.

References

- [1] Chuang Hu, Wei Bao, Dan Wang, and Fengming Liu. Dynamic Adaptive DNN Surgery for Inference Acceleration on the Edge. In *IEEE International Conference on Computer Communications (INFOCOM)*. IEEE, 2019.
- [2] Surat Teerapittayanon, Bradley McDanel, and HT Kung. Distributed Deep Neural Networks over the Cloud, the Edge and End Devices. In *2017 IEEE 37th International Conference on Distributed Computing Systems (ICDCS)*, pages 328–339. IEEE, 2017.
- [3] Seungyeop Han, Haichen Shen, Matthai Philipose, Sharad Agarwal, Alec Wolman, and Arvind Krishnamurthy. MCDNN: An Approximation-Based Execution Framework for Deep Stream Processing under Resource Constraints. In *Proceedings of the 14th Annual International Conference on Mobile Systems, Applications, and Services (MobiSys)*, pages 123–136. ACM, 2016.
- [4] Ji Wang, Jianguo Zhang, Weidong Bao, Xiaomin Zhu, Bokai Cao, and Philip S Yu. Not Just Privacy: Improving Performance of Private Deep Learning in Mobile Cloud. In *Proceedings of the 24th ACM SIGKDD International Conference on Knowledge Discovery & Data Mining*, pages 2407–2416. ACM, 2018.
- [5] Qingchen Zhang, Laurence T Yang, and Zhikui Chen. Privacy Preserving Deep Computation Model on Cloud for Big Data Feature Learning. *IEEE Transactions on Computers*, 65(5):1351–1362, 2016.
- [6] Reza Shokri, Marco Stronati, Congzheng Song, and Vitaly Shmatikov. Membership Inference Attacks against Machine Learning Models. In *IEEE Symposium on Security and Privacy (SP)*, pages 3–18. IEEE, 2017.
- [7] Karan Ganju, Qi Wang, Wei Yang, Carl A Gunter, and Nikita Borisov. Property Inference Attacks on Fully Connected Neural Networks using Permutation Invariant Representations. In *Proceedings of the 2018 ACM SIGSAC Conference on Computer and Communications Security (CCS)*, pages 619–633. ACM, 2018.
- [8] Luca Melis, Congzheng Song, Emiliano De Cristofaro, and Vitaly Shmatikov. Exploiting Unintended Feature Leakage in Collaborative Learning. In *IEEE Symposium on Security and Privacy (SP)*. IEEE, 2019.
- [9] Zhibo Wang, Mengkai Song, Zhifei Zhang, Yang Song, Qian Wang, and Hairong Qi. Beyond Inferring Class Representatives: User-Level Privacy Leakage From Federated Learning. In *Proc. IEEE International Conference on Computer Communications (INFOCOM)*. IEEE, 2019.
- [10] Alexey Dosovitskiy and Thomas Brox. Inverting Visual Representations with Convolutional Networks. In *Proceedings of the IEEE Conference on Computer Vision and Pattern Recognition (CVPR)*, pages 4829–4837, 2016.
- [11] Matthew D Zeiler and Rob Fergus. Visualizing and Understanding Convolutional Networks.
- [12] Aravindh Mahendran and Andrea Vedaldi. Understanding Deep Image Representations by Inverting Them. In *Proceedings of the IEEE conference on computer vision and pattern recognition (CVPR)*, pages 5188–5196, 2015.
- [13] Reza Shokri and Vitaly Shmatikov. Privacy-Preserving Deep Learning. In *Proceedings of the 22nd ACM SIGSAC conference on computer and communications security*, pages 1310–1321. ACM, 2015.
- [14] Martin Abadi, Andy Chu, Ian Goodfellow, H Brendan McMahan, Ilya Mironov, Kunal Talwar, and Li Zhang. Deep Learning with Differential Privacy. In *Proceedings of the 2016 ACM SIGSAC Conference on Computer and Communications Security*, pages 308–318. ACM, 2016.
- [15] Nicolas Papernot, Martín Abadi, Ulfar Erlingsson, Ian Goodfellow, and Kunal Talwar. Semi-Supervised Knowledge Transfer for Deep Learning from Private Training Data. *international conference on learning representations (ICLR)*, 2017.
- [16] Payman Mohassel and Yupeng Zhang. Secureml: A System for Scalable Privacy-Preserving Machine Learning. In *2017 IEEE Symposium on Security and Privacy (SP)*, pages 19–38. IEEE, 2017.
- [17] Payman Mohassel and Peter Rindal. ABY 3: a Mixed Protocol Framework for Machine Learning. In *Proceedings of the 2018 ACM SIGSAC Conference on Computer and Communications Security*, pages 35–52. ACM, 2018.
- [18] Jun Zhang, Zhenjie Zhang, Xiaokui Xiao, Yin Yang, and Marianne Winslett. Functional Mechanism: Regression Analysis under Differential Privacy. *Proceedings of the VLDB Endowment*, 5(11):1364–1375, 2012.
- [19] Nicholas D Lane and Petko Georgiev. Can Deep Learning Revolutionize Mobile Sensing? In *Proceedings of the 16th International Workshop on Mobile Computing Systems and Applications*, pages 117–122. ACM, 2015.

- [20] Jianfeng Chi, Emmanuel Owusu, Xuwang Yin, Tong Yu, William Chan, Yiming Liu, Haodong Liu, Jiasen Chen, Swee Sim, Vibha Iyengar, et al. Privacy partition: A privacy-preserving framework for deep neural networks in edge networks. In *2018 IEEE/ACM Symposium on Edge Computing (SEC)*, pages 378–380. IEEE, 2018.
- [21] Anand Padmanabha Iyer, Li Erran Li, Mosharaf Chowdhury, and Ion Stoica. Mitigating the Latency-Accuracy Trade-off in Mobile Data Analytics Systems. In *Proceedings of the 24th Annual International Conference on Mobile Computing and Networking (MobiCom)*, pages 513–528. ACM, 2018.
- [22] Biyi Fang, Xiao Zeng, and Mi Zhang. NestDNN: Resource-Aware Multi-Tenant On-Device Deep Learning for Continuous Mobile Vision. In *Proceedings of the 24th Annual International Conference on Mobile Computing and Networking (MobiCom)*, pages 115–127. ACM, 2018.
- [23] Song Han, Huizi Mao, and William J Dally. Deep Compression: Compressing Deep Neural Networks with Pruning, Trained Quantization and Huffman Coding. *International Conference on Learning Representations (ICLR)*, 2016.
- [24] Anubhav Ashok, Nicholas Rhinehart, Fares Beainy, and Kris M. Kitani. N2N learning: Network to Network Compression via Policy Gradient Reinforcement Learning. *International Conference on Learning Representations (ICLR)*, 2018.
- [25] Sicong Liu, Yingyan Lin, Zimu Zhou, Kaiming Nan, Hui Liu, and Junzhao Du. On-Demand Deep Model Compression for Mobile Devices: A Usage-Driven Model Selection Framework. In *Proceedings of the 16th Annual International Conference on Mobile Systems, Applications, and Services (MobiSys)*, pages 389–400. ACM, 2018.
- [26] Zhou Wang, Alan C Bovik, Hamid R Sheikh, Eero P Simoncelli, et al. Image Quality Assessment: from Error Visibility to Structural Similarity. *IEEE transactions on image processing*, 13(4):600–612, 2004.
- [27] Geoffrey Hinton, Oriol Vinyals, and Jeff Dean. Distilling the Knowledge in a Neural Network. *stat*, 1050:9, 2015.
- [28] Ronald J Williams. Simple Statistical Gradient-Following Algorithms for Connectionist Reinforcement Learning. *Machine learning*, 8(3-4):229–256, 1992.